Chemical Engineering Journal 162 (2010) 809–820

Contents lists available at ScienceDirect

Chemical Engineering Journal

journal homepage: www.elsevier.com/locate/cej

Computer-aided biocompatible solvent design for an integrated extractive fermentation–separation process

Hou-Chieh Cheng, Feng-Sheng Wang*

Department of Chemical Engineering, National Chung Cheng University, 168 University Rd., Min-Hsiung, Chia-Yi 621-02, Taiwan

ARTICLE INFO

Article history:
Received 8 February 2010
Received in revised form 10 June 2010
Accepted 12 June 2010

Keywords:
Solvent design
Extractive fermentation
Extractive distillation
CAMD
Fuzzy optimization
Evolutionary computation

ABSTRACT

Computer-aided process/solvent design is introduced to find a feasible biocompatible solvent for an extractive fermentation and separation process. The designed biocompatible solvent serves as both the extractant for extractive fermentation and the entrainer for extractive distillation, to yield water-free ethanol. Several goals, such as maximizing production rate and extraction efficiency, and limiting solvent utilization, are simultaneously considered in the optimal solvent design problem. Thus, the design was formulated as a mixed-integer nonlinear optimization problem. A two-phase computational scheme was introduced to solve the problem. The mixed-integer hybrid differential evolution (MIHDE) algorithm was first applied to solve the problem in order to obtain a feasible solution. The feasible solution was then served as an initial starting point for the mixed-integer sequential quadratic programming (MISQP) solver to numerically confirm that the optimal design was achieved. We have compared the crisp and fuzzy approaches to the design problem. The fuzzy goal attainment approach is able to address goal trade-offs and yield an overall satisfactory grade for the problem.

1. Introduction

Bioethanol is a bulk chemical that is often produced by integrated fermentation and separation processes. Such an integrated process for bioethanol production typically involves two major steps: (1) enhancement of the bioethanol production rate; (2) recovery and purification of the bioethanol from the dilute fermentation liquor. Achieving high ethanol production rate requires high-cell concentration in the fermentor and maximizing the dilution rate. Continuous fermentation can increase the production rate [1–6]; however, it cannot be carried out with high-cell-density cultures, which results in low ethanol concentration and a significant loss of residual substrate. To increase the efficiency of the ethanol fermentation process, various cell culture methods have been investigated. Continuous fermentation with cell recycling has received considerable interest in recent years as a method for achieving higher ethanol concentration [7–11]. However, high ethanol concentration may poison viable microorganisms and hinder the fermentation process. Extractive fermentation is an alternative technique used to reduce inhibition of the end-product, which is ethanol in this study, by removing the fermentation product *in situ* [12–17]; however, the toxicity of the organic solvent used to remove the product is always a problem [17–21]. Non-biocompatible organic solvent could be poisonous to microbes resulted in inactivity. Several reports have taken advantages of computer-aided molecular design (CAMD) to design biocompatible solvents for extractive fermentation [17–19,22–26].

Distillation is a traditional method for recovering and purifying ethanol from dilute fermentation liquor. The liquor is first distilled by using heat to concentrate the ethanol up to 192 proof (96 wt%). Molecular sieves are then used to remove the remaining water, resulting in 200 proof ethanol (100.0 wt%). In recent years, extractive distillation has gained widespread acceptance in industrial chemical plants [27,28]. Extractive distillation is a vapor–liquid process that uses a third component to achieve a chemical separation. In the case of an azeotropic ethanol/water mixture, the extractive agent (referred to as the entrainer) enhances the volatility difference between the mixture components. The solvent can then be recovered and reused. The solvent can serve as both the entrainer in extractive distillation and the extractant in extractive fermentation to reduce the total operating cost; however, such a solvent should satisfy physical and chemical criteria for both fermentation and separation processes.

CAMD techniques have been successfully applied for designing various types of solvents, including extraction solvents [16–19,22–24,29–33], absorption solvents [25,26,34–36], distillation solvents [37,38], reaction solvents [39], and crystallization solvents [40]. These techniques can be classified in terms of their solution algorithm into generate and test approaches, and optimization-based approaches. Generate and test approaches [29,31,33,37,39] are based on the formation of all possible molecular structures from a specified set of building groups and the

* Corresponding author. Tel.: +886 5 2720411x33404; fax: +886 5 2721206.
E-mail address: chmfsw@ccu.edu.tw (F.-S. Wang).

1385-8947/$ – see front matter © 2010 Elsevier B.V. All rights reserved.
doi:10.1016/j.cej.2010.06.018

Nomenclature

b_r	bleed ratio for the cell recycle unit
$Conv_{ov}$	overall substrate conversion
D_0	dilution rate for the fed substrate (h^{-1})
D_E	dilution rate based on the effluent solvent flow rate (h^{-1})
D_R	dilution rate based on the influent and effluent solvent flow rate at the first extractive fermentor, respectively (h^{-1})
D_s	dilution rate based on the influent solvent flow rate (h^{-1})
EE	extraction efficiency (%)
K_e	ethanol distribution coefficient
K_p	saturation coefficient for cell growth on ethanol
K_{pI}	inhibition coefficient for cell growth on ethanol
K_s	saturation coefficient for cell growth on glucose
K_{sI}	inhibition coefficient for cell growth on glucose
L_{C50}	the lethal concentration causing 50% mortality in fathead minnow (mol/L)
M_{W_j}	molecular weight for $j = e$ (ethanol), s (solvent) and w (water)
P_E	ethanol concentration in extractive phase (g/L)
P_R	ethanol concentration in raffinate phase (g/L)
S_0	fed substrate concentration (g/L)
S_E	glucose concentration in extractive phase (g/L)
S_R	glucose concentration in raffinate phase (g/L)
T_b	boiling point for the solvent
T_f	melting point for the solvent
ΔG	Gibbs free energy for the solvent
x_e^E	mole fraction of ethanol in extractive phase
x_s^E	mole fraction of solvent in extractive phase
x_e^R	mole fraction of ethanol in raffinate phase
x_s^R	mole fraction of solvent in raffinate phase

Greek letters

μ	specific growth rate of *Saccharomyces diastaticus* LORRE 316
μ_{max}	maximum specific growth rate (h^{-1})
δ_l	contribution of group l in group contribution-based model for L_{C50}
β_i	flow rate ratio between influent dilution rate and effluent aqueous flow rate for the ith extractive fermentor
η	the overall solvent selectivity (w/w)
γ_{ij}^E	activity coefficient of component j in extractive phase for the ith extractive fermentor
γ_{ij}^R	activity coefficient of component j in raffinate phase for the ith extractive fermentor
ν_j	valence of group j
π_v	overall mass flow rate of fresh solvent (g/h L)
ρ_v	density of solvent (g/L)

screening of the generated molecules according to molecular design feasibility rules and preselected target physical property values. In optimization approaches [18,19,22–26,30,32,35,36,40], optimal molecular structures are founded out by formulating and solving an optimization problem which is generally expressed as mixed-integer mathematical programming problems. Many literature reports of optimization-based CAMD problems only consider a single objective to the design problem. Traditionally, process design and solvent molecular design have been treated as two separate problems, with little or no feedback between the two approaches. Each problem has been conveniently isolated or decoupled from the other. Multiobjective optimization approaches [25,41–44] can indeed combine both process and solvent molecular design problems in order to determine an optimal solvent structure and to optimize the specifications of process performances simultaneously. This approach has certain advantages over a single objective optimal design that can achieve a compromised result for the integrated processes.

In this study, we will apply the optimization-based CAMD approach to determine a biocompatible solvent to suit for the integrated extractive fermentation and distillation process. A biocompatible criterion of this CAMD problem requires that the solvent used to extract ethanol from the continuous fermentation process be nontoxic solvent to microorganisms [18]. Maximization of extraction efficiency is also a key consideration; however, higher extraction efficiencies require much more solvent utilization. Many performance specifications should be considered to yield a trade-off solution. A fuzzy or flexible optimization approach is applied to design a biocompatible solvent for the integrated extractive fermentation process using interval restriction. The resulting biocompatible solvent serves as both the extractant for the extractive fermentation and the entrainer for the extractive distillation, ultimately yielding water-free bioethanol. Moreover, the crisp optimization approach is also discussed to compare the results from the flexible approach.

2. Problem formulation

2.1. Description of the integrated process

In this study, we design a novel biocompatible solvent that serves as both the extractant for removing ethanol from the fermentation liquor, to prevent ethanol-mediated inhibition, and as the entrainer for extractive distillation, to yield water-free bioethanol. The integrated extractive fermentation and distillation process is shown in Fig. 1. The solvent is added to the fermentor to extract ethanol, preventing product inhibition. The integrated fermentation process consists of a stirred-tank extractive fermentor with a cell separator, used to filter and recycle the microbes back into the fermentor to enhance the production rate. The fermented liquor is then transformed to the extractive distillation process to yield water-free ethanol and to recover the solvent. The extractive fermentation is assumed to be operated in a chemostat, and the ethanol is maintained in a state of liquid-liquid equilibrium at the operating temperature $T = 308$ K and pressure $P = 1$ atm. Fresh substrate is continuously fed into the fermentor, and the cell-free extractive stream flows into the extractive distillation column. The solvent affects the volatility of the ethanol/water azeotope such that the water becomes the distillate in the rectifying section of the extractive distillation column. The bottom stream of the extractive distillation column flows into the second column for solvent recovery and production of water-free ethanol.

The aim of the study focuses on designing a biocompatible solvent to serve as the extractant for extractive fermentation and the entrainer for extractive distillation. We apply a separate or decomposition approach to find the optimal solvent molecular structure and the operation conditions for the extractive fermentation process that is to simultaneously maximize ethanol production rate and extractive efficiency with subject to process and solvent constraints. The relative volatility is also considered as an additional measure in the solvent design problem. We consider that the relative volatility should be greater than the assigned bound value so that the designed biocompatible solvent is then served as an entrainer for the extractive distillation in order to yield water-free ethanol.

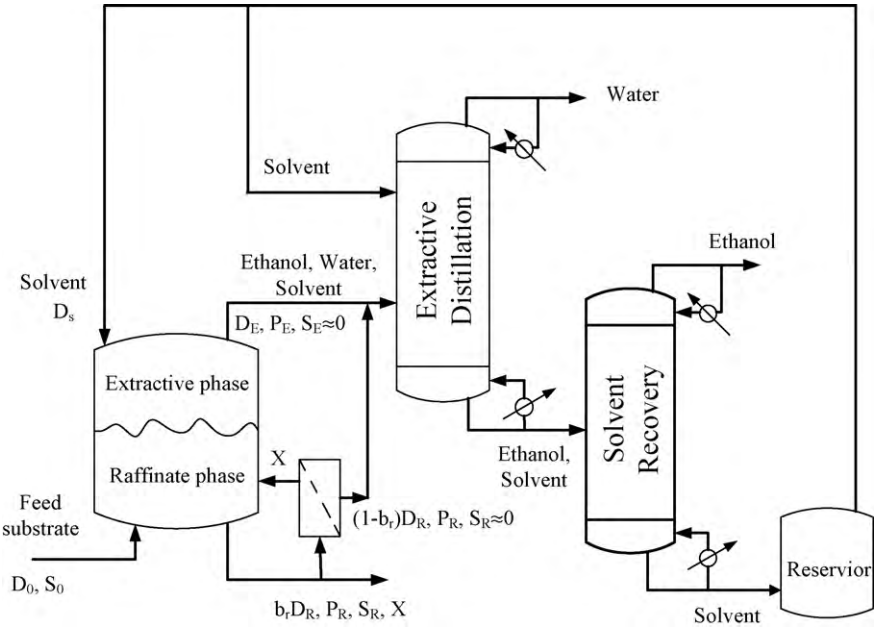

Fig. 1. An integrated continuous extractive fermentation–distillation processes.

2.2. Process constraints

In the study, the extractive and raffinate phases in the fermentor are assumed to be in phase equilibrium. Using the steady-state material balance for yeast under slightly aerobic condition, we obtain that the aqueous dilution rate in the raffinate phase is equal to the specific growth rate μ of the yeast, expressed in the following form:

$$D_R = \frac{1}{b_r}\mu \tag{1}$$

where b_r is the bleed ratio of the cell recycle unit and μ is the specific growth rate of a yeast. The specific growth rate was taken from Wang and Sheu [45], that was used the yeast, *Saccharomyces diastaticus* LORRE 316, to produce ethanol under slightly aerobic condition. As a result, the formulation of the specific growth rate was in terms of glucose and ethanol concentrations, but not included the dissolved oxygen, as expressed in the form:

$$\mu = \frac{\mu_m S_R}{K_S + S_R + S_R^2/K_{sI}} \frac{K_P}{K_p + P_R + P_R^2/K_{pI}} \tag{2}$$

where $\mu_m = 0.4721\,h^{-1}$ is the coefficient of the growth rate (h^{-1}), $K_s = 27.9036$ g/L is glucose saturation constant (g/L), $K_{sI} = 213.5899$ g/L is the glucose inhibition constant (g/L), $K_p = 27.9036$ g/L is the ethanol saturation constant (g/L), $K_{pI} = 41.2979$ is the ethanol inhibition constant (g/L), and S_R and P_R are the aqueous substrate and ethanol concentrations (g/L) in the raffinate phase, respectively.

The steady-state material balances for glucose and ethanol can be rearranged to form the equality constraint:

$$\frac{D_R P_R + D_E P_E}{D_0 S_0 - D_R S_R - D_E S_E} = \hat{Y}_{ps} \tag{3}$$

where S_0 is the fed substrate concentration (g/L), S_E and P_E are the substrate concentration (g/L) and ethanol concentration (g/L) in the extractive phase, respectively, and D_E is the dilution rate based on the effluent solvent flow rate (h^{-1}). In this case study, the yield factor is $\hat{Y}_{ps} = 0.4721$. The dilution rate (D_0, h^{-1}) for the fed substrate is defined as $D_0 = (1/\beta)D_R$, where β is the flow rate ratio.

2.3. Solvent constraints

The aim of this study is to apply an optimization-based CAMD methodology to design a biocompatible solvent for the integrated extractive fermentation processes. Some physical, chemical, and biological solvent requirements need to be specified for the CAMD problem. For predicting liquid phase splitting, we assume that the process streams from the extractive and raffinate phases in the extractive fermentor are in phase equilibrium such that the activity coefficients, γ_i^E and γ_i^R, can be calculated by the UNIFAC method [46]. For extractive fermentation, the relationships of phase equilibrium for each component are therefore expressed as follows:

$$\gamma_i^E x_i^E = \gamma_i^R x_i^R, \quad i = e\,(\text{ethanol}), s\,(\text{solvent}), w\,(\text{water}) \tag{4}$$

where x_i^E and x_i^R, are the mole fractions of ethanol, solvent and water in the extractive and raffinate phases, respectively, for the extractive fermentor. We assume that the process streams from the extractive and raffinate phases in the fermentor are in phase equilibrium such that the ethanol distribution coefficient, K_e, the solvent selectivity, η, and the solvent loss, ζ, in raffinate phase can be calculated as follows [32]:

$$K_e = \frac{\gamma_e^R}{\gamma_e^E}\frac{MW_w}{MW_s} \tag{5}$$

$$\eta = \frac{\gamma_w^E}{\gamma_e^E}\frac{MW_e}{MW_w} \tag{6}$$

The octet rule, modeled by Odele and Macchietto [35], is employed to ensure that the resulting solvent molecule is structurally feasible. The acyclic octet rule is expressed as follows:

$$\sum_{i=1}^{N_{\max}} (2 - \nu_j)u_{ji} = 2, \quad j = 1, \ldots, M \tag{7}$$

where $N_{\max}$ is the maximum number of available positions in a molecule, ν_j is the valence of group j, M is the number of available groups in the basis, and the binary variable u_{ji} is defined as:

$$u_{ji} = \begin{cases} 1, & \text{if the structural group } j \text{ appear in } i\text{th position of a molecule} \\ 0, & \text{otherwise} \end{cases} \tag{8}$$

While the structure of a molecule is selected, the biocompatibility ($-\log L_{C50}$, mol/L), the boiling point (T_b, K), the melting point (T_f,

Table 1
Alcohol, alkane, ketone, ether and ester components selected to evaluate the corresponding relative volatilities, biocompatibilities and boiling points.

Alcohol	Alkane	Ketone	Ester	Ether
1-Undecanol, $C_{11}H_{24}O$	Dodecane, $C_{12}H_{26}$	1-Undecanone, $C_{11}H_{22}O$	n-Octyl acetate, $C_{10}H_{20}O_2$	Hexyl ether, $C_{12}H_{26}O$
1-Decanol, $C_{10}H_{22}O$	Undecane, $C_{11}H_{24}$	2-Decanone, $C_{10}H_{20}O$	Heptyl acetate, $C_9H_{18}O_2$	Methyl nonyl ether, $C_{10}H_{22}O$
1-Nonanol, $C_9H_{20}O$	Decane, $C_{10}H_{22}$	2-Nonanone, $C_9H_{18}O$	Hexyl ethanoate, $C_8H_{16}O_2$	Hexyl methyl ether, $C_7H_{16}O$
1-Octanol, $C_8H_{18}O$	Nonane, C_9H_{20}	1-Octanone, $C_8H_{16}O$	Amyl acetate, $C_7H_{14}O_2$	
1-Heptanol, $C_7H_{16}O$	Octane, C_8H_{18}	2-Heptanone, $C_7H_{14}O$	n-butyl acetate, $C_6H_{12}O_2$	

K), and the Gibbs free energy (ΔG, KJ/mol) can be evaluated by the group contribution method. Moreover, the possible values need to be restricted to yield a suitable solvent. These inequality constraints are expressed as follows:

$$-\log L_{C50} = \sum_j \sum_i u_{ji}\delta_j \le B_{L_{C50}} \tag{9}$$

$$T_b^L \le T_b = 198 + \sum_j \sum_i u_{ji} T_{bj} \le T_b^U \tag{10}$$

$$T_f = 122.5 + \sum_j \sum_i u_{ji} T_{fj} \le T_f^U \tag{11}$$

$$\Delta G = 583.57 - \sum_j \sum_i u_{ji} \Delta G_j > 0 \tag{12}$$

where T_{bj}, T_{fj}, and ΔG_j are the boiling point, melting point and Gibbs free energy for the contributions of group j, respectively, and can be calculated from the literature [47]. Quantitatively estimating biocompatibility can be difficult since there are not many experimental data available regarding the toxicity contribution for each group to microbes; thus, the criterion used for fathead minnow is employed to cope with biocompatibility for microbes [18]. Thus, it is supposed that the behaviors of microbes are the same as those of fathead minnow and the toxicity contribution for each group δ_l to fathead minnow is the same as that for microbes [48]. Using the group contribution approach, the toxicity of a selected solvent is summed up to its contributed value. Here, L_{C50} is the lethal concentration that causes 50% mortality in microbes. The bound values for the biocompatibility (B_{LC50}), the boiling point ($[T_b{}^L, T_b{}^U]$), and the melting point ($T_f{}^U$) are assigned by the designer. The lower bound of the melting point ($T_f{}^U$) is needed to ensure that the solvent is in the liquid state at the necessary operating conditions.

The aim of this study is to design a novel biocompatible solvent for the extractive fermentation that also uses as the entrainer for the extractive distillation to yield water-free ethanol. We consider the relative volatility of the ethanol and water mixture as a measure for determining a suitable entrainer that is able to destroy the azeotrope of the mixture. The relative volatility, $\alpha_{e/w}$, is restricted as follows:

$$\alpha_{e/w} = \frac{\gamma_w^E}{\gamma_e^E}\frac{P_w^{vp}}{P_e^{vp}} \ge \alpha_{e/w}^U \tag{13}$$

where P_w^{vp} and P_e^{vp} are the vapor pressures of water and ethanol, respectively. The relative volatility must be greater than the bound value $\alpha_{e/w}^U$ to avoid azeotrope formation.

The bound values expressed in (9)–(13) must be assigned in advance to find a suitable solvent. Alcohol, alkane, ketone, ether and ester are the commonly used molecular groups used in the design of biocompatible solvents for extractive fermentation [22–24]. The designed solvent should have a high relative volatility to facilitate the recovery of solvent and yield water-free ethanol in the extractive distillation. In this study, we first searched for candidate molecules for alcohol, alkane, ketone, ether and ester with molecular weight between 100 and 200 g/M from the chemical database (http://webbook.nist.gov/chemistry/) in order to estimate the bound values. Table 1 lists the components selected from each group: alcohol, alkane, ketone, ether and ester, to compute the corresponding relative volatilities, as shown in Fig. 2a. The relative volatility for each candidate ether is less than the value of two, suggesting low separation efficiencies and an inability to achieve

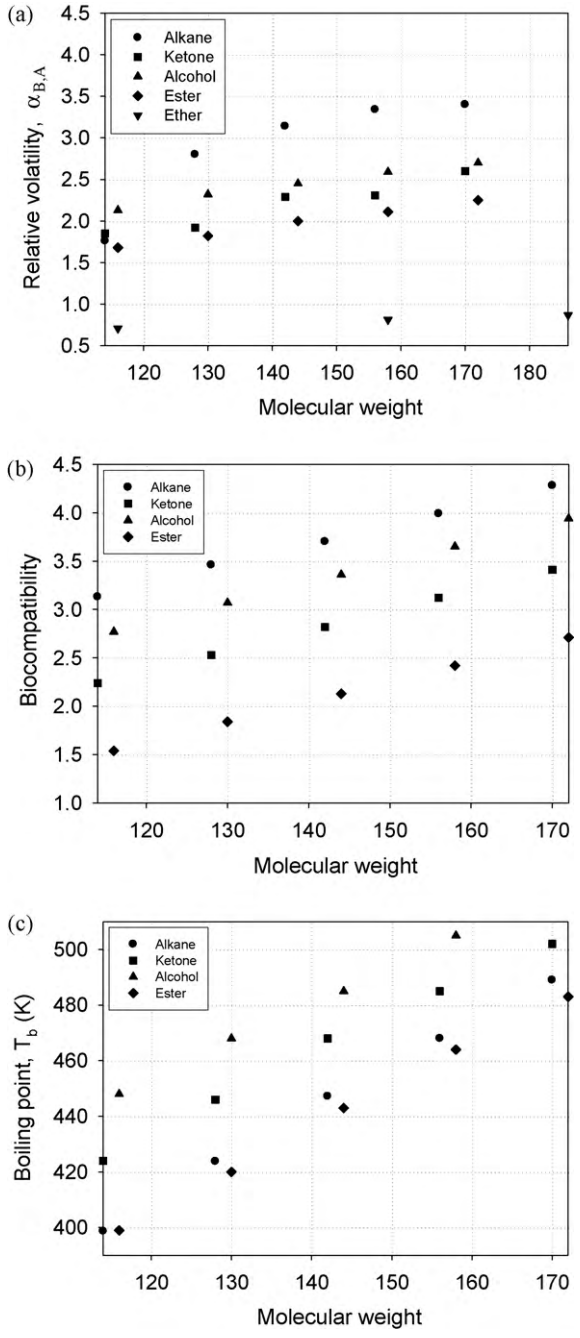

Fig. 2. Solvent screening for the extractive fermentation/extractive distillation problem.

the desired specifications for extractive distillation. Accordingly, the group basis set can exclude ether in order to easily fulfil the inequality constraint (14) during evolutionary search. Therefore, we chose the group basis set as $\mathbf{u}$ = [CH_3, CH_2, CH, OH, CH_3COO, CH_2COO, CH_3CO, CH_2CO] for construction of an optimal solvent molecule.

Fig. 2b and c shows the biocompatibilities and the boiling points, respectively, for each group: alcohol, alkane, ester and ketone. Dodecanol had been applied to extract ethanol *in situ* from a fermentation process [15] and is the toxic solvent, with a biocompatibility of 4.25 mol/L. Thus, we assigned a biocompatibility bound (B_{LC50}) of 3.5 mol/L to find a less toxic solvent. Based on Fig. 2c, the lower and upper bounds for the boiling point were assigned as 401 K and 501 K. The upper bound for the melting point was set to 288 K, such that the selected solvent will remain in the liquid state during extractive fermentation.

3. Optimal design

3.1. Crisp design specifications

The process formulation and constraints of the integrated fermentation process have been described in the previous section. We next consider maximizing the ethanol production rate as the design objective for determining a biocompatible solvent for the integrated process. The single objective function is therefore expressed as follows:

$$\max_{y,u} f_1 = \text{Prod} = D_E P_E + D_R P_R \tag{14}$$

where the process operation vector $\mathbf{y}$ consists of the dilution rates, D_S and D_E, based on influent and effluent solvent flow rates, respectively, the flow rate ratio, β, and the bleed ratio, b_r. The integer vector $\mathbf{u} \in \{1, \ldots, 8\}$ is used to represent each molecular group in the group basis set, [CH_3, CH_2, CH, OH, CH_3COO, CH_2COO, CH_3CO, CH_2CO], for selecting solvent molecular structure. The optimization problem becomes a mixed-integer nonlinear programming (MINLP) problem, which consists of real-value variables for determining process operations and integer variables for selecting the solvent molecular structure from the group basis set.

The extraction efficiency, solvent utilization rate and conversion are three additional criteria used in investigating the performance of the design problem. Higher extraction efficiencies indicate that the selected solvent is more efficient for the given process. The extraction efficiency is therefore defined as the ratio of the ethanol recovered in the solvent phase to ethanol production:

$$EE = \frac{D_E P_E}{D_E P_E + D_R P_R} \geq M_E^L \tag{15}$$

where M_E^L is the desired value for ethanol extraction efficiency and is provided by the designer. An extraction efficiency of one indicates that ethanol is completely removed from the fermentor. In contrast, a value of zero indicates that the selected solvent is unable to extract any ethanol from the fermented liquor.

To minimize operating costs, the designer should use as little solvent as possible for the integrated process. The solvent utilization rate is obtained from the ratio of the equilibrium composition, and is restricted as follows:

$$D_s \rho_s = \left(K_e \frac{x_s^E}{x_e^E} D_E + \frac{x_s^R}{x_e^R} D_R \right) \frac{P_R}{MW_e} MW_s \leq M_s^U \tag{16}$$

where D_s is the dilution rate based on the influent solvent flow rate, ρ_s is the solvent density, and M_s^U is the upper bound for the mass flow rate of solvent and is provided by the designer. Glucose conversion is another criterion for bioreactor performance analysis. We stipulated that the conversion should be greater than the desired value, $Conv^L$, as follows:

$$Conv = 1 - \frac{D_R S_R}{D_0 S_0} - \frac{D_E S_E}{D_0 S_0} \geq Conv^L \tag{17}$$

3.2. Flexible design specifications

The single objective design problem under the crisp environment described thus far is referred to as the crisp-preference design problem. This problem indicates that the designer has not assigned a preference goal for the ethanol production rate and the boundary for each constraint; or alternatively, the designer has assigned the goal and boundaries, but the optimal solvent and its corresponding operating conditions must absolutely satisfy both the rigid goal and the boundaries. However, in practical applications, the goal and the boundary for each constraint are, in general, interval boundaries, not a rigid value. Additionally, many optimal design problems can be formulated as multiobjective optimization problems (MOOP) to allow for flexible decision making. Two requirements must be satisfied in the decision-making problem. The first requirement is to solve the MOOP to obtain the optimal operating variables and the associated optimal objective function values and constraints. The second requirement is to check whether each optimal objective function value and constraints satisfies the pre-assigned goals and boundaries. If any optimal objective function value does not satisfy the goals or any constraints are violated, then the designer must make compromises with respect to some goals and boundaries and repeat the problem to obtain a satisfactory solution. Some preference techniques, such as nonlinear goal programming, compromise programming and surrogate worth trade-off methods, can be employed to solve the decision-making problem. However, such methods can only be used to solve problems with crisp preferred goals, but are not suited for interval-constraint boundaries. In this study, we will apply a fuzzy goal attainment method to overcome such drawbacks.

In the preference design problem, the designer usually assigns an interval goal, rather than a rigid value. Here, we consider the interval goal for the production rate $[f_1^L, f_1^U]$ and for the extraction efficiency $[f_2^L, f_2^U]$, respectively. The preference goal problem is therefore expressed as follows:

$$\widetilde{\max_{y,u}} f_1 = \text{Prod} \gtrsim [f_1^L, f_1^U] \tag{18}$$

$$\widetilde{\max_{y,u}} f_2 = EE \gtrsim [f_2^L, f_2^U] \tag{19}$$

where $[f_k^L, f_k^U]$, k = 1,2 are the preference intervals, which are provided by the designer. The symbol "$\widetilde{\max}$" denotes flexible or fuzzy maximization. Here, the symbol "$\gtrsim$" denotes a relaxed or fuzzy version of the ordinary inequality "$\geq$". The fuzzy maximization means that the design is completely acceptable if the production rate and extraction efficiency are greater than each corresponding upper bound f_k^U. Conversely, the design is completely unacceptable if the maximum production rate and extraction efficiency are less than the lower bound f_k^L. When the production rate and extraction efficiency are within the intervals $[f_k^L, f_k^U]$, $k = 1, 2$, it is implied that the design has some degree of satisfaction.

The fuzzy optimal design problem is also included with the solvent utilization rate as a flexible or fuzzy inequality constraint:

$$f_3 = D_s \rho_s \precsim [f_3^L, f_3^U] = [M_s^L, M_s^U] \tag{20}$$

where the symbol "$\precsim$" denotes a fuzzy or flexible version of the ordinary inequality "$\leq$", and $[f_3^L, f_3^U]$ is the interval boundary for the solvent mass flow rate. The fuzzy inequality constraint means that the design is completely acceptable if the mass flow rate of solvent is less than M_s^L. Conversely, the design is completely unacceptable if D_s ρ_s is greater than M_s^U. When the solvent mass flow rate of is

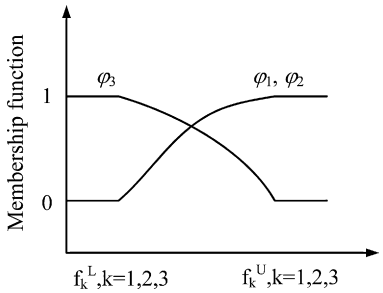

Fig. 3. The monotonically increasing membership functions for ethanol production rate (φ_1) and extraction efficiency (φ_2), and monotonically decreasing function for the solvent utilization rate (φ_3).

within $[M_s^L, M_s^U]$, it is implied that the design is satisfactory to some degree.

The fuzzy goal for each objective function can be quantified by eliciting membership functions from the designer. In maximization, a fuzzy goal stated by the designer may be to achieve "substantially greater than or equal to some interval", and the designer is asked to determine the subjective membership function, which is a strictly monotonically increasing function with respect to f_k:

$$\varphi_k(f_k) = \begin{cases} 0; & f_k \le f_k^L, \quad k = 1, 2 \\ d_k; & f_k^L \le f_k \le f_k^U \\ 1; & f_k^U \le f_k \end{cases} \tag{21}$$

where f_k^L and f_k^U represents the value of f_k such that the grade of the membership function $\varphi_k(f_k)$ is 0 or 1 and the grades of the membership for the intermediate function values are expressed by a strictly monotonically increasing function d_k with respect to f_k. For concise presentation for the fuzzy optimization problem, the membership functions for both objectives are supposed to be identical, as shown in Fig. 3. For treating the fuzzy inequality constraint, we propose the following membership function:

$$\varphi_3(f_3) = \begin{cases} 1, & f_3 \le f_3^L \\ d_3', & f_3^L \le f_3 \le f_3^U \\ 0, & f_3 \ge f_3^U \end{cases} \tag{22}$$

where f_3^L and f_3^U represents the value of f_3 such that the grade of the membership function $\varphi_3(f_3)$ is 1 or 0 and the grades of the membership for the intermediate function values are expressed by a strictly monotonically decreasing function d_3' with respect to f_3. The membership function for the inequality constraint is also shown in Fig. 3.

How to choose the membership functions those depend on the designer's preference. Sakawa [49] proposed using five types of membership functions: linear, exponential, hyperbolic inverse and piecewise linear functions. For concise illustration of fuzzy optimization problems, the exponential membership functions for each objective function and inequality constraint are shown in Fig. 3. The membership level for each objective and constraint is between zero and one. The zero level indicates that the designer is completely unsatisfactory to the corresponding goal. In contrast, the grade is acquired to one if the value for each goal is 100% satisfactory. From Fig. 3, we observe that the membership functions for the objectives are dual to those of the inequality constraints. As a result, the fuzzy optimization is to find a compromised solution from these goals. If both objective functions and the inequality constraint are less than their lower bounds, that means we acquire the membership function value of zero for the objective function and one for the inequality constraints. The intersection for these membership functions is zero. Conversely, if both objective functions and the inequality constraint are greater than the upper bounds, the intersection for these membership functions is still zero. The aim of fuzzy optimization is therefore to find a maximum intersection for all membership functions between the desired boundaries.

Having elicited the membership functions from the designer for each objective function and constraint, the flexible optimization problem can be expressed as a fuzzy goal attainment problem in the following form:

$$\min_{z\in\Omega}\varphi_D = \min_{z\in\Omega}\left[\max_{k=1,2,3}\{\bar{\varphi}_k - \varphi_k(f_k)\} + \delta\sum_{k=1}^{3}(\bar{\varphi}_k - \varphi_k(f_k))\right] \tag{23}$$

where φ_D denotes an aggregation function and the search domain Ω for the crisp constraints in (3), (9)–(13) and (17). Several aggregation functions are introduced in a textbook by Sakawa [49]. The value of the aggregation function can be interpreted as a representation of the overall degree of satisfaction with the designer's fuzzy goals. The first term of the aggregation function is applied to determine the optimal trade-off solution that is nearest to the ideal preference goal $\bar{\varphi}_k$, which indicates 100% satisfaction. The second term is employed to avoid inspection of a unique test for optimality, in which the constant δ is a sufficiently small positive value of 10^{-3}–10^{-5}.

3.3. Computational strategy

This optimal design problem (23) is a mixed-integer nonlinear programming (MINLP) problem, which consists of real-value variables for determining process operating conditions and integer variables for selecting the solvent structure. The computational flowchart is shown in Fig. 4. In this work, we apply mixed-integer hybrid differential evolution (MIHDE) [50–52] to solve the MINLP problem and obtain an optimal solvent and its corresponding operating conditions. The MIHDE algorithm extends from the real-value version of hybrid differential evolution (HDE) introduced by Chiou and Wang [53]. The real coding strategy cannot handle MINLP problems. Lin et al. [51,52] have introduced a mixed-coding strategy for HDE, which has been applied to several chemical process design problems. The MIHDE can use a small population size to find an optimal solution. In MIHDE, four setting factors are required to be set as follows: the crossover factor was set to 0.5. The two tolerances used in the migration operation were set to 0.05. A population size of five was used in MIHDE for all runs. Each individual consists of the process operation variables and molecular selection variables. The integer variables generated from MIHDE, as shown in Fig. 4, are first applied to select a solvent molecular structure, and then the selected solvent is combined with the process operation variables represented as real-valued variables in MIHDE to compute the process, chemical and physical constraints. Such data are then applied to compute the membership function values for the objectives and constraints. The aggregation function in (23) is severed as the fitness function for MIHDE to generate the next better individuals towards obtaining an optimal solution. Fig. 4 can be also applied to solve the crisp optimization problem that the objective function value and constraints are directly used to evaluate the fitness value for each individual in the MIHDE algorithm.

Determination of global optimal solution for the MINLP problems has been one of the major thrust areas in recent years [54–58]. Global optimization techniques can be classified as deterministic and stochastic approaches. Deterministic approaches like branch and bound, cutting plane and decomposition schemes guarantee convergence for a given level of accuracy. The success of a deterministic method, e.g. branch-and-bound like methods, is critically dependent on the successful solution and optimality of the nonlinear programming (NLP) at each node. The available standard NLP solvers may get stuck at local optima or may even fail to solve the NLP problem at the local node. Recently some alternate approaches that modify deterministic branch-and-bound algo-

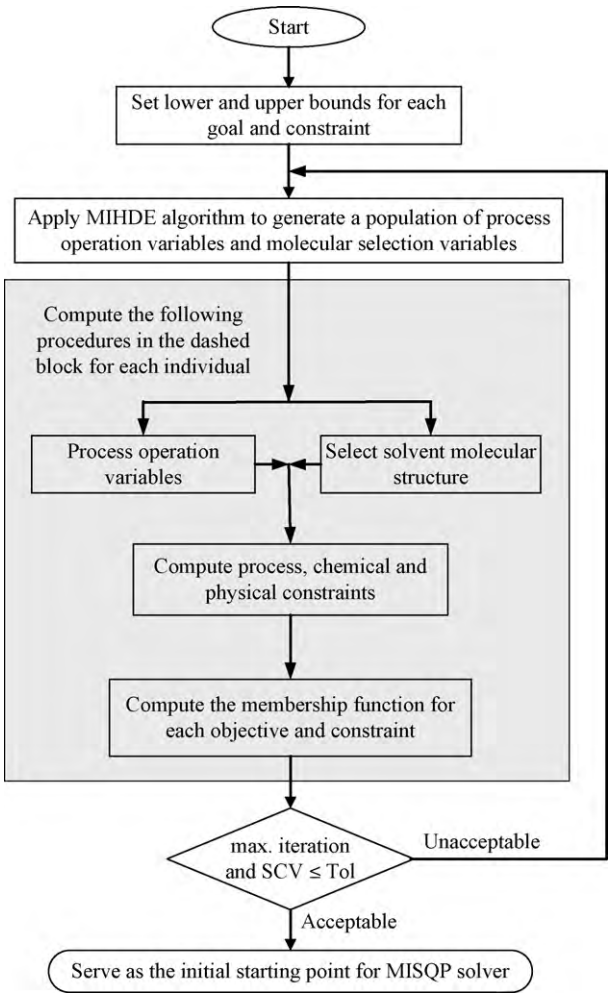

Fig. 4. Computational flowchart for the two-phase algorithm for crisp and fuzzy solvent design problems. The first phase is to apply MIHDE as a search engine to find a near optimal solution, and then the solution is used as the starting point for MISQP solver to obtain the refined solution in order to numerically validate optimality for the solution.

rithms towards solution to global optimality have been proposed. These approaches are based on relaxation, partitioning and bounding steps that result in an evolutionary refinement of the search space [54–58]. On the other hand, stochastic approaches, such as genetic algorithms [59–62], MIHDE [50–53], and simulated annealing [26,32,42,44], do not make any assumptions about the nature of the convexity of the objective function and constraints. Though genetic algorithms or MIHDE are often slow and do not guarantee convergence, they have been widely used in numerous applications and may have high probability to yield global optimal solutions to complex problems. Handling of integer variables is relatively easier and the solution is generally unaffected by the presence of nonlinear terms involving discrete variables. In this study, we introduce two-phase computational schemes to solve the MINLP problem. The first phase, as shown in Fig. 4, is applied MIHDE to find a feasible solution, which may be an optimal solution or a near optimal solution for the process/solvent design problem. The feasible solution is then served as the initial starting point for a trust region sequential quadratic programming algorithm [56–58], namely MISQP, to numerically confirm that the feasible solution obtained by MIHDE is an optimal solution if the MISQP solver converges and achieves the nearly identical solution. The detailed computational procedures will be discussed in the next section.

Penalty function methods represent one of the most popularly used techniques in evolutionary algorithms to manage constraints [59]. However, penalty function methods have certain weaknesses that can become serious when the penalty parameters are too large. Such a situation makes the penalty function ill conditioned so that it is difficult to achieve an optimal solution. Lin et al. [52] have proposed an adaptive penalty parameter strategy into the MIHDE with a multiplier updating method to enforce global convergence for constrained MINLP problems. In the present work, we applied MIHDE with a multiplier updating method, including an adaptive penalty parameter strategy to solve the optimal process/solvent design problem. The initial penalty parameters were set to 10^3 for all runs. In the computations, we use the sum of the constraint violations (SCV) to inspect the feasibility of the optimal solution. SCV was defined as:

$$\mathrm{SCV} = \sum |g_e| + \sum \max\{0, g_i\} \tag{24}$$

The first term in Eq. (24) indicates the sum of the equality constraint violations, and the second one is the sum of inequality constraint violations. This equation indicates that an optimal solution with a smaller SCV is a more feasible solution to the problem.

4. Results and discussion

4.1. Crisp optimal design

The crisp optimal design problem is only considered in terms of maximization of ethanol production rate. The bound values in (9)–(13) for the solvent properties were discussed in the previous section. The bound values in (15)–(17) for the operating restrictions are assigned as follows: the lower bound for the extraction efficiency is 70%, the upper bound for the mass flow rate of solvent is 1000 g/h L, and the lower bound for the conversion is 0.8. The optimal result for the first run is listed in Table 2. The optimal solvent molecular structure contains three CH_3 groups, two CH_2 groups, one CH group, and one CH_2CO group. This structure is referred to as 3-methyl-5-heptanone, which is identified by CAS registry number as 541-85-5. The resulting maximum ethanol production rate is 27.86 g/h L. The solvent selectivity, biocompatibility and relative volatility were 14.7 w/w, 2.96 and 2.2, respectively. Other physical properties are listed in the first run of Table 2.

Supposing that the designer intends to enhance the ethanol extraction efficiency, the crisp optimal design problem should be solved again. For the crisp optimization approach, the designer has to carry out a series of trade-off procedures towards solving optimal solvent design problems, such as to tighten or to loosen the limits for some constraints in the optimization problem, and then to solve each problem in order to yield a series of optimal designs. The interactive procedure is repeated until achieving a compromised design. From Eqs. (14) and (15), we observe that higher ethanol extraction efficiency inherently results in deceasing ethanol production rate. We sequentially increased the bound value for the extractive efficiency to 80 and 90%, respectively, and then each optimization problem was solved by MIHDE to yield a trade-off table, as shown in Run 2 and Run 3 of Table 2. For Run 2 and Run 3 we obtained the same solvent, which the optimal solvent molecular structure contains three CH_3 groups, one CH_2 groups, one CH group, and one $-CH_2CO$ group. This structure is referred to as isoamyl methyl ketone, which is identified by CAS registry number as 110-12-3. The ethanol production rate decreased to 15.2 g/h L for Run2 and 10.42 g/h L for Run 3, which decreased 45% and 63% compared to the first run.

The fourth and fifth runs in Table 2 suppose that the designer aims to use less solvent utilization rate, with bound values of 850 and 700 g/h L, respectively. According to the designer requirements,

Table 2
Crisp optimal design for the integrated extractive fermentation–distillation process.

Run	M_E^L (%)	M_s^U (g/h L)	Solvent structure	K_e (w/w)	η (w/w)	ζ (wt%)	$\alpha_{w/e}$	$-\log L_{C50}$	T_b (K)	T_f (K)	*Conv* (%)	D_s ρ_s (g/Lh)	EE (%)	max f_1 (g/h L)	SCV	CPU Time (h)
1	70	1000	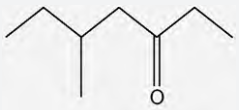	0.37	14.7	2.97e−3	2.2	2.96	435.9 (432.7)[a]	214.9	99.8	1000.0	70.0	27.86	8.90e−10	4.47
2	80	1000	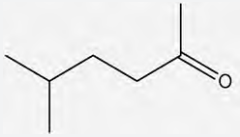	0.41	13.3	66.17e−3	2.0	2.67	413.0 (415 ± 7)[a]	203.6 (199.3)[a]	81.0	1000.0	82.0	15.20	1.29e−9	5.04
3	90	1000	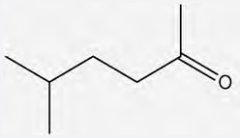	0.52	13.6	5.85e−3	2.0	2.67	413.0 (415 ± 7)[a]	203.6 (199.3)[a]	99.9	1000.0	90.0	10.42	8.70e−10	4.73
4	70	850	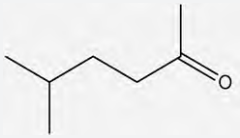	0.43	13.6	5.85e−3	2.0	2.67	413.0 (415±7)[a]	203.6 (199.3)[a]	99.9	850.0	90.0	8.86	6.79e−10	4.38
5	70	700	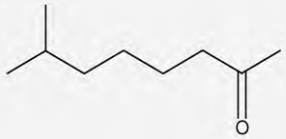	0.43	13.3	1.66e−3	2.0	3.25	458.8 (NA)	226.1 (NA)	80.0	700.0	90.8	4.79	1.13e−8	4.37

NA: not available.
[a] Data was accessed from NIST Chemistry WebBook (http://webbook.nist.gov/chemistry/).

Table 3
Flexible optimal design for integrated extractive fermentation–distillation processes.

Item	Case 1	Case 2	Case 3
S_0 (g/L)	250	325	400
Solvent structure	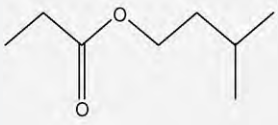	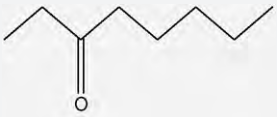	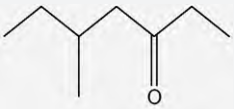
f_1^* (g/h L)	13.17	18.60	20.99
f_2^* (%)	77.0	81.7	83.7
f_3^* (g/h L)	930.0	883.5	862.9
$\varphi_1(f_1^*)$	0.329	0.509	0.580
$\varphi_2(f_2^*)$	0.329	0.509	0.580
$\varphi_3(f_3^*)$	0.329	0.509	0.580
Conv (%)	99.8	99.9	99.9
K_e (w/w)	0.29	0.40	0.42
η (w/w)	13.5	14.9	14.6
ζ (wt%)	0.0014	0.0028	0.0030
$-\log L_{C50}$	2.6	2.54	2.96
$\alpha_{w/e}$	2.02	2.24	2.19
T_b (K)	440.2 (433.2)	436.31 (439 ± 3)[a]	435.9 (432.7)[a]
T_f (K)	207.3	229.85	214.9
D_R (h^{-1})	0.11	0.12	0.10
D_E (h^{-1})	1.25	1.3	1.26
β	0.96	0.96	0.92
b_r	0.03	0.14	0.06
SCV	3.00e−12	3.93e−12	3.61e−13
CPU time (h)	4.14	4.50	5.74

[a] Data was accessed from NIST Chemistry WebBook (http://webbook.nist.gov/chemistry/).

both crisp optimization problems were solved by MIHDE. The optimal results are also shown in Table 2. For Run 4, the optimal solvent molecular structure is identical to Run 2. For Run 5, the optimal solvent molecular structure contains two CH_3 groups, four CH_2 groups, one CH group, and one CH_3CO group. This structure is referred to as 7-methyl-2-octanone, which is identified by CAS registry number as 1482-13-9. The ethanol production rate decreased 5.8-fold compared to the first run. The SCV value for each run is very small that indicates each solution is feasible.

4.2. Flexible optimal design

An optimal design problem is generally a decision-making problem that requires using interactive procedures to obtain a compromised result if the designer would like to determine the other satisfactory designs. For the crisp optimization approach, the designer needs to carry out the interactive procedures towards solving a series of optimization design problems as discussed in the previous section (see Table 2) in order to obtain a compromised design. Generally speaking, the designer has a preferred goal for the objective and a preferred limit for each constraint in practical optimization problems. Such goal and limits are rather interval boundaries. The flexible optimization technique can be applied to alleviate such an interactive computational burden and to consider all preferred objectives and constraints simultaneously in order to obtain the compromised solution among the preference intervals. To solve the flexible goal attainment problem (23), we used the exponential membership function shown in Fig. 3 to judge the degree of satisfaction for ethanol production rate, extraction efficiency and solvent utilization rate. The lower and upper bounds were 5 and 40 g/h L for ethanol production rate, 70 and 100% for extraction efficiency, and 700 and 1000 g/h L for the solvent utilization rate. The optimal results obtained by MIHDE are shown in the first case of Table 3. The optimal solvent structure consists of three CH_3 groups, two CH_2 groups, one CH group and one CH_2COO group. This structure corresponds to iospentyl propionate, which is identified by the CAS registry numbers as 105-68-0. The maximum ethanol production rate and extractive efficiency were 13.17 g/L and 77%, respectively, which correspond to the nearly identical satisfactory grades of 0.329. The solvent utilization rate was 930 g/h L, which also corresponds to a satisfactory grade of 0.329. The fuzzy goal attainment approach is capable of determining a trade-off result from the interval goals and constraints. The overall satisfactory grade was 0.329 in this case. The optimal process operating conditions and physical properties obtained by this approach are also shown in Table 3.

The fed substrate concentration, S_0, was maintained at 250 g/L in the first case. Higher fed concentration should enhance ethanol production rate. Therefore, we increased the fed substrate concentration to 325 and 400 g/L, respectively, to determine the corresponding optimal design. The optimal results obtained by MIHDE are presented in Case 2 and Case 3 of Table 3, respectively. For Case 2, the optimal solvent molecular structure consists of two CH_3 group, four CH_2 groups and one $-CH_2CO$ group. Such a structure is referred to as 3-octanone which is identified by CAS registry number as 106-68-3. For Case 3, the optimal solvent molecular structure contains three CH_3 groups, two CH_2 groups, one CH group, and one CH_2CO group. This structure is as same as that obtained from the crisp optimization as shown in Run 1 of Table 2. The overall satisfactory grade was 0.509 for Case 2 and 0.580 for Case 3. The overall satisfactory grade is enhanced with increasing substrate concentration. However, 3-octanone has a little bit higher relative volatility suggesting that it is easier to recover in extraction distillation.

4.3. Solvent recovery

The designed biocompatible solvents serve as both the extractant for the extractive fermentation and as the entrainer for the extractive distillation, to yield water-free bioethanol. The relative volatility is considered as a design specification in the solvent design problem, so that the relative volatility $\alpha_{w/e}$ for each optimal solvent is greater than 2.0, as shown in Tables 2 and 3. This restriction means that the designed solvent can be applied for extractive

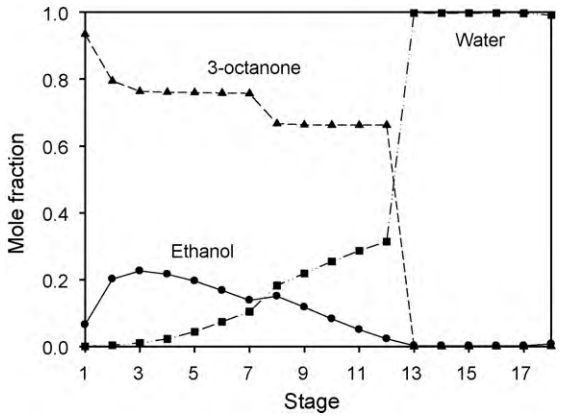

Fig. 5. Mole fraction distributions for each component in the extractive distillation column using 3-octanone that is obtained from the flexible optimal solution using the fed substrate concentration of 325 g/L.

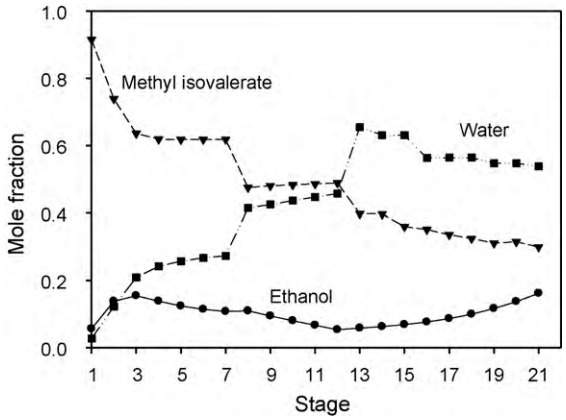

Fig. 6. Mole fraction distributions for each component in the extractive distillation column using methyl isovalerate that is obtained from Cheng and Wang [24].

distillation to obtain nearly water-free ethanol. The optimal solvents shown in Table 2 and 3 were each applied to the extractive distillation process, using the UNIFAC method, to evaluate their separation ability. For the sake of brevity, we only show the computational results using 3-octanone as the entrainer fed to the extractive distillation column. Fig. 5 shows the mole fraction distributions for each component in the extractive distillation column, using 18 stages and a reflux ratio of 2.14. The stream from the fermentor and the fresh solvent stream are fed to the 7th and 12th stage, respectively. In this case, the distillate flow rate is 6.12 mol/h. Fig. 5 shows that the water is distilled to the top of the extractive distillation column, and the solvent and ethanol flow to the bottom of the distillation column. From Fig. 5, it is observed that the distillate is almost all water. In contrast, the mole fractions of ethanol, water and 3-octanone at the bottom of the extractive distillation column are 6.52, 0.05 and 93.43 mol%, respectively. The mole fraction of the remaining water in the bottoms is lower than the standard of 1.28 mol%. The bottoms are then fed into the solvent recovery tower to recover the solvent and yield water-free ethanol.

Cheng and Wang [24] reported an optimal biocompatible for single and double extractive fermentation processes, although restriction of the relative volatility was not included in the optimal design problem. In such a case study, methyl isovalerate is also applied to investigate the separation performance in the extractive distillation process. Following similar procedures as described above, the mole fraction distributions for each stage are shown in Fig. 6. The stream from the fermentor and the fresh solvent stream are fed at the 7th and 12th stage, respectively. The distillate flow rate is the same as in the previous case. The water is distilled to the top of the extractive distillation column; however, the distillate does not only yield water. The mole fractions of ethanol, water and methyl isovalerate at the top of the extractive distillation column are 16.2, 53.82 and 29.98 mol%, respectively. In contrast, the mole fractions for ethanol, water and methyl isovalerate at the bottom of the extractive distillation column are 5.65, 2.76 and 91.59 mol%,

Table 4
Flexible optimal design solved by MISQP using the starting integer variables obtained from the optimal molecular structures for each case study in Table 3.

Item	MISQP-Case1	MISQP-Case2	MISQP-Case3
S_0 (g/L)	250	325	400
Solvent structure	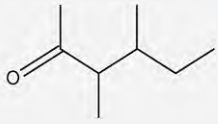	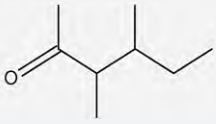	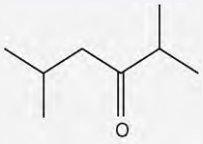
f_1^* (g/h L)	2.44	1.74	2.23
f_2^* (%)	83.8	86.1	85.4
f_3^* (g/h L)	911.1	1000.0	790.5
$\varphi_1(f_1^*)$	0.0	0.0	0.0
$\varphi_2(f_2^*)$	0.582	0.656	0.634
$\varphi_3(f_3^*)$	0.406	6.22e−7	0.795
Conv (%)	96.1	87.4	99.5
K_e (w/w)	0.06	0.06	0.07
η (w/w)	11.3	13.3	14.6
ζ (wt%)	6.75	6.98	6.83
$-\log L_{C50}$	3.39	3.39	3.39
$\alpha_{w/e}$	1.7	2.0	2.2
T_b (K)	435.43 (431.2)[a]	435.43 (431.2)[a]	435.43 (420.7)[a]
T_f (K)	199.85	199.85	199.85
D_R (h^{-1})	0.02	0.01	0.01
D_E (h^{-1})	1.31	1.43	1.13
β	0.71	0.98	0.98
b_r	0.20	0.16	0.17
SCV	5.97e−1	2.29e−10	7.68e−11

[a] Data was accessed from NIST Chemistry WebBook (http://webbook.nist.gov/chemistry/).

respectively. The mole fraction of the remaining water in the bottoms is greater than the standard value; thus, methyl isovalerate is unsuitable as an entrainer for extractive distillation.

4.4. Numerical comparison

In the first computational phase, we have applied the MIHDE algorithm to solve crisp and fuzzy optimization problems, respectively. In the second computational phase, we applied the Fortran subroutine MISQP, which is provided by Professor Schittkiwski, to solve the optimization problems. For concise explanation, we show the results for the fuzzy goal attainment problem only. The MISQP solver is a trust region sequential quadratic programming algorithm and has succeeded to solve several mixed-integer nonlinear programming problems [56–58]. The default values for real options and integer options in MISQP are used to solve the problems. The integer variables are used to represent the eight molecular groups. As a result, they are unable to be relaxed as real numbers in solving progress. The nearest integer option in MISQP is used to select the corresponding molecular group. The fuzzy goal attainment problem is a non-differentiable min–max problem, which can be directly solved by MIHDE. However, when MISQP is applied to solve the problem, it has to be converted into a smooth one by adding one additional variable and three inequality constraints. The solution quality for MISQP depends on the assigned starting values. In the computations, we have first carried out 20 runs for solving the solvent design problem by MISQP with using randomly starting values. By using such randomly starting values, a feasible solution is incapable to achieve because the acyclic octet rule in Eq. (8) is unable to meet. We next use the solvent obtained from Cases 1, 2 and 3 in Table 3 as the starting integer values, but starting real values are randomly generated. Table 4 shows each convergent result obtained by MISQP using the corresponding starting value. The optimal solvents are 3,4-dimethyl-2-hexanone for Cases 1 and 2, and isobutyl isopropyl for Case 3. Both Cases 2 and 3 are the local optimal solutions because the SCV of 2.29e−10 and 7.68e−11 are very small. However, both production rates are about one-tenth smaller than those obtained from MIHDE as shown in Cases 2 and 3 of Table 3. For Case 1, we obtained the premature solution, because both material balance equation (3) and relative volatility constraint (13) are unsatisfied. We also use each optimal result obtained from Table 3 as the starting integer and real values for MISQP in order to solve each problem. MISQP can obtain the complete identical designs to those of MIHDE, except the SCV of 2.27e−9, 2.36e−8 and 3.81e−9, respectively. This numerical validation is shown that the results of Table 3 obtained by MIHDE are the optimal solutions.

5. Conclusions

In this study, the relative volatility restriction is introduced in the solvent design problem to find the optimal solvent molecular structure and the operation conditions for the extractive fermentation process. The design problem was formulated as a mixed-integer nonlinear programming problem to design a novel biocompatible solvent that serves as the extractant, to remove ethanol from the fermented liquor and prevent ethanol inhibition, and also as the entrainer for the extractive distillation, to yield the water-free bioethanol. CAMD problems are generally considered with a single objective in an optimal design problem. For practical applications, however, several goals should be simultaneously satisfied in the optimal design problem. The flexible optimization approach is more convenient technique than the crisp approach to design a biocompatible solvent for the integrated extractive fermentation/distillation process for ethanol production. In the crisp approach, the designer has to apply an interactive computational procedure, as shown in Table 2, to find a satisfactory solution. However, the interval goals and constraints are assigned by the designer in advance, and are directly applied for the flexible optimization problem to determine an optimal solution through the goal attainment method. The goal attainment method is to find a satisfactory solution of the Pareto frontier. Moreover, the degree of satisfaction for each objective function and constraint could be obtained from the solution. The designed biocompatible solvent serves as both the extractant the extractive fermentation and the entrainer for extractive distillation, to yield water-free ethanol. In this solvent design problem, we considered the performance for the extractive fermentation process only that is to find the optimal solvent molecular structure and the operation conditions to simultaneously maximize ethanol production rate and extractive efficiency with subject to process and solvent constraints. The economical and environmental issues have been applied as design criteria to evaluate the integrated solvent and process design [25,41–44]. Such criteria can be used as alternative measured indexes to the integrated extractive fermentation and distillation process.

Acknowledgments

Financial support from the National Science Council, Taiwan, ROC (Grant NSC97-2221-E-194-010-MY3 and NSC96-2221-E-194-024), is greatly appreciated. The authors would like to thank Professor Schittkiwski, Department of Computer Science at University of Bayreuth, Germany, to provide the MISQP subroutine for evaluating the problem.

References

[1] D.P. Bayrock, W.M. Ingledew, Application of multistage continuous fermentation for production of fuel alcohol by very-high-gravity fermentation technology, J. Ind. Microbiol. Biotechnol. 27 (2001) 87–93.
[2] Y.H. Lin, D. Bayrock, W.M. Ingledew, Metabolic flux variation of *Saccharomyces cerevisiae* cultivated in multistage continuous stirred tank reactor fermentation environment, Biotechnol. Prog. 17 (2001) 1055–1060.
[3] R.K. Warren, G.A. Hill, D.G. Macdonald, Improved bioreaction kinetics for the simulation of continuous ethanol fermentation by *Saccharomyces cerevisiae*, Biotechnol. Prog. 6 (1990) 319–325.
[4] S.D. Watt, H.S. Sidhu, M.I. Nelson, A.K. Ray, Analysis of a model for ethanol production through continuous fermentation, Anziam J. 49 (2007) C85–C99.
[5] H. Kuriyama, H. Ishibashi, H. Miyagawa, H. Kobayashi, E. Mikami, Optimization of two-stage continuous ethanol fermentation using flocculating yeast, Biotechnol. Lett. 15 (1993) 415–420.
[6] N.M. Faqir, M.M. Attarakih, Optimum design of a series of CSTRs performing reversible Michaelis-Menten kinetics: a rigorous mathematical study, Bioprocess Eng. 20 (1999) 329–335.
[7] G.H. Gil, W.J. Jones, T.G. Tornabene, Continuous ethanol production in a two-stage, immobilized/suspended-cell bioreactor, Enzyme Microb. Technol. 13 (1991) 390–399.
[8] K. Kargupta, S. Datta, S.K. Sanyal, Analysis of the performance of a continuous membrane bioreactor with cell recycling during ethanol fermentation, Biochem. Eng. J. 1 (1998) 31–37.
[9] A. Nishiwaki, I.J. Dunn, Performance of a multistage fermentor with cell recycle for continuous ethanol production, Chem. Eng. Commun. 162 (1997) 179–198.
[10] A. Nishiwaki, I.J. Dunn, Analysis of a two-stage fermentor with recycle for continuous ethanol production, Chem. Eng. Commun. 168 (1998) 207–227.
[11] T.H. Park, J. Hong, H.C. Lim, Teoretical analysis of the effect of cell recycling on recombinant cell fermentation processes, Biotechnol. Prog. 7 (1991) 77–84.
[12] A.J. Daugulis, D.B. Axford, P.J. McLellan, Economics of ethanol production by extractive fermentation, Can. J. Chem. Eng. 69 (1991) 488–497.
[13] M. Gyamerah, J. Glover, Production of ethanol by continuous fermentation and liquid-liquid extraction, J. Chem. Technol. Biotechnol. 66 (1996) 145–152.
[14] W. Kang, R. Shukla, K.K. Sirkar, Ethanol production in a microporous hollow-fiber-based extractive fermentor with immobilized yeast, Biotechnol. Bioeng. 36 (1990) 826–833.
[15] F. Kollerup, A.J. Daugulis, A mathematical model for ethanol production by extractive fermentation in a continuous stirred tank fermentor, Biotechnol. Bioeng. XXVII (1985) 1335–1346.
[16] R.D. Offeman, S.K. Stephenson, G.H. Robertson, J.O. William, Solvent extraction of ethanol from aqueous solutions. I. Screening methodology for solvents, Ind. Eng. Chem. Res. 44 (2005) 6789–6796.
[17] M.J. Chen, F.S. Wang, Optimal trade-off design of integrated fermentation processes for ethanol production using genetically engineered yeast, Chem. Eng. J. 158 (2010) 271–280.

[18] Y. Wang, L.E.K. Achenie, Computer aided solvent design for extractive fermentation, Fluid Phase Equilibr. 201 (2002) 1–18.
[19] Y. Wang, L.E.K. Achenie, A hybrid global optimization approach for solvent design, Comp. Chem. Eng. 26 (2002) 1415–1425.
[20] H. Kapucu, Ü. Mehmetoğlu, Strategies for reducing solvent toxicity in extractive ethanol fermentation, Appl. Biochem. Biotechnol. 75 (1998) 205–214.
[21] V.M. Yabannavar, D.I.C. Wang, Strategies for reducing solvent toxicity in extractive fermentations, Biotechnol. Bioeng. 37 (1991) 716–722.
[22] H.C. Cheng, F.S. Wang, Trade-off optimal design of a biocompatible solvent for an extractive fermentation process, Chem. Eng. Sci. 62 (2007) 4316–4324.
[23] H.C. Cheng, F.S. Wang, Optimal biocompatible solvent design for a two-stage extractive fermentation process with cell recycling, Comp. Chem. Eng. 32 (2008) 1385–1396.
[24] H.C. Cheng, F.S. Wang, Optimal process/solvent design for ethanol extractive fermentation with cell recycling, Biochem. Eng. J. 41 (2008) 258–265.
[25] A.I. Papadopoulos, P. Linke, Multiobjective molecular design for integrated process-solvent systems synthesis, AIChE J. 52 (2005) 1057–1070.
[26] A.I. Papadopoulos, P. Linke, Efficient integration of optimial solvent and process design using molecular clustering, Chem. Eng. Sci. 61 (2006) 6316–6336.
[27] I.D. Gil, A.M. Uyazán, J.L. Aguilar, L.A. Rodrígurez, Caicedo, Separation of ethanol and water by extractive distillation with salt and solvent as entrainer: process simulation, Braz. J. Chem. Eng. 25 (2008) 207–215.
[28] E.L. Ligero, T.M.K. Ravagnani, Dehydration of ethanol with salt extractive distillation – a comparative analysis between processes with salt recovery, Chem. Eng. Process. 42 (2003) 543–552.
[29] R. Gani, E.A. Brignole, Molecular design of solvents for liquid extraction based on UNIFAC, Fluid Phase Equilibr. 13 (1983) 331–340.
[30] A. Giovanoglou, J. Barlatier, C.S. Adjiman, E.N. Pistikopoulos, J.L. Cordiner, Optimal solvent design for batch separation based on economic performance, AIChE J. 49 (2003) 3095–3109.
[31] M. Hostrup, P.M. Harper, R. Gani, Design of environmentally benign processes: integration of solvent design and separation process synthesis, Comp. Chem. Eng. 23 (1999) 1395–1414.
[32] E.C. Marcoulaki, A.C. Kokossis, On the development of novel chemicals using a systematic optimization approach. Part II. Solvent design, Chem. Eng. Sci. 55 (2000) 2547–2561.
[33] E.J. Pretel, P.A. Lopez, S.B. Bottini, E.A. Brignole, Computer-aided molecular design of solvents for separation processes, AIChE J. 40 (1994) 1349–1360.
[34] M.R. Eden, S.B. Jørgensen, R. Gani, M.M. El-Halwagi, A novel framework for simultaneous separation process and product design, Chem. Eng. Process. 43 (2004) 595–608.
[35] O. Odele, S. Macchietto, Computer aided molecular design: a novel method for optimal solvent selection, Fluid Phase Equilibr. 82 (1993) 47–54.
[36] E.N. Pistikopoulos, S.K. Stefanis, Optimal solvent design for environmental impact minimization, Comp. Chem. Eng. 22 (1998) 717–733.
[37] B. Chen, Z. Lei, Q. Li, C. Li, Application of CAMD in separating hydrocarbons by extractive distillation, AIChE J. 51 (2005) 3114–3141.
[38] B. van Dyk, I. Nieuwoudt, Design of solvents for extractive distillation, Ind. Eng. Chem. Res. 39 (2000) 1423–1429.
[39] R. Gani, C. Jiménez-González, D.J.C. Constable, Method for selection of solvents for promotion of organic reactions, Comp. Chem. Eng. 29 (2005) 1661–1676.
[40] A.T. Karunanithi, L.E.K. Achenie, R. Gani, A computer-aided molecular design framework for crystallization solvent design, Chem. Eng. Sci. 61 (2006) 1247–1260.
[41] K.J. Kim, U.M. Diwekar, Integrated solvent selection and recycling for continuous processes, Ind. Eng. Chem. Res. 41 (2002) 4479–4488.
[42] A.I. Papadopoulos, P. Linke, A unified framework for integrated process and molecular design, Chem. Eng. Res. Design 83 (A6) (2005) 674–678.
[43] A.I. Papadopoulos, P. Linke, A decision support grid for integrated molecular solvent design and chemical process selection, Comp. Chem. Eng. 33 (2009) 72–87.
[44] A.I. Papadopoulos, P. Linke, Integrated solvent and process selection for separation and reactive separation systems, Chem. Eng. Process.: Process Intensification 48 (2009) 1047–1060.
[45] F.S. Wang, J.W. Sheu, Multiobjective parameter estimation problems of fermentation processes using a high ethanol tolerance yeast, Chem. Eng. Sci. 55 (2000) 3685–3695.
[46] J. Gmehling, P. Rasmussen, A. Fredenslund, Vapor liquid equilibria by using UNIFAC group contribution. Revision and extension 2, Ind. Eng. Chem. Process Design Dev. 21 (1982) 118–127.
[47] K.G. Joback, R.C. Reid, Estimation of pure-component properties from group-contributions, Chem. Eng. Commun. 57 (1987) 233–243.
[48] C. Gao, R. Govind, H.H. Tabak, Application of the group contribution method for predicting the toxicity of organic chemicals, Environ. Toxicol. Chem. 11 (1992) 631–636.
[49] M. Sakawa, Fuzzy Sets and Interactive Multiobjective Optimization, Plenum Press, New York, 1993.
[50] C.T. Liao, W.J. Tzeng, F.S. Wang, Mixed-integer hybrid differential evolution for synthesis of chemical processes, J. Chin. Inst. Chem. Eng. 32 (2001) 491–502.
[51] Y.C. Lin, K.S. Hwang, F.S. Wang, Co-evolutionary hybrid differential evolution for mixed-integer optimization problems, Eng. Optim. 33 (2001) 663–682.
[52] Y.C. Lin, K.S. Hwang, F.S. Wang, Evolutionary Lagrange method for mixed-integer constrained optimization problems, Eng. Optim. 35 (2003) 267–284.
[53] J.P. Chiou, F.S. Wang, Hybrid method of evolution algorithms for static and dynamic optimization problems with application to a fedbatch fermentation process, Comp. Chem. Eng. 23 (1999) 1277–1291.
[54] G.M. Ostrovsky, L.E.K. Achenie, M. Sinha, A reduced dimension branch-and-bound algorithm for molecular design, Comp. Chem. Eng. 27 (2003) 551–567.
[55] C.A. Floudas, Nonliner and Mixed-Integer Optimization, Oxford University Press, Oxford, 1995.
[56] O. Exler, K. Schittkowski, A trust region SQP algorithm for mixed-integer nonlinear programming, Optim. Lett. 1 (2007) 269–280.
[57] O. Exler, T. Lehmann, K. Schittkowski, MISQP: A Fortran Implementation of a Trust Region SQP Algorithm for Mixed-Integer Nonlinear Programming: User's Guide, Report, Department of Computer Science, University of Bayreuth, Germany, 2009.
[58] K. Schittkowski, A Collection of 100 Test Problems for Nonlinear Mixed-Integer Programming in Fortran, Report, Department of Computer Science, University of Bayreuth, Germany, 2009.
[59] Z. Michalewicz, M. Schoenauer, Evolutionary algorithms for constrained parameter optimization problems, Evol. Comput. 4 (1996) 1–32.
[60] S.A. Munawar, R.D. Gudi, A nonlinear transformation based hybrid evolutionary method for MINLP solution, Chem. Eng. Res. Design 83 (A10) (2005) 1218–1236.
[61] I.R.S. Victorino, J.P. Maia, E.R. Morais, M.R. Wolf Maciel, R. Maciel Filho, Optimization for large scale process based on evolutionary algorithms: genetic algorithms, Chem. Eng. J. 132 (2007) 1–8.
[62] X. Chen, N. Wang, A DNA based genetic algorithm for parameter estimation in hydrogenation reaction, Chem. Eng. J. 150 (2009) 527–535.